Available online at www.sciencedirect.com

ScienceDirect

Procedia Structural Integrity 42 (2022) 722–729

Structural Integrity Procedia

www.elsevier.com/locate/procedia

23 European Conference on Fracture - ECF23

Nickel-Titanium peripheral stents: can fracture mechanics shed light on their fatigue failure?

Francesca Berti[a], Alma Brambilla[a,b], Roberto Porcellato[a,b], Luca Patriarca[b], Lorenza Petrini[c]*

[a]*LaBS-Department of Chemistry, Materials and Chemical Engineering "G. Natta", Politecnico di Milano, Piazza Leonardo da Vinci 32, Milano 20133, Italy*

[b]*Department of Mechanical Engineering, Politecnico di Milano, Via La Masa 1, Milano 20156, Italy*

[c]*Department of Civil and Environmental Engineering, Politecnico di Milano, Piazza Leonardo da Vinci 32, Milano 20133, Italy*

Abstract

The major concern about Nickel-Titanium (Ni-Ti) stents, which are the gold standard in the treatment of occlusive peripheral disease, is fatigue and the consequent fracture in vivo. Indeed, their failure might be responsible for severe drawbacks, among which is the re-occlusion of the treated artery. Although many phenomenological approaches have been proposed to study this topic, the current literature lacks extensive knowledge on the Ni-Ti local damage mechanisms produced by the cyclic loads that promote crack nucleation and lead to the failure of thin struts, such as those of stents. Moreover, due to the super-elastic property of the alloy, the standard approach for interpreting the fracture of metals might be not accurate for this case. This work aims at increasing awareness of fatigue failure in superelastic Ni-Ti thin struts, such as those of stents. To do so, multi-wire specimens, sharing the same dimensions and thermo-mechanical treatment of the stent struts, were fatigue tested under different strain levels and the number of cycles to failure was recorded for each sample. Numerical simulations corroborated the experimental results to gain information on the local stress and strain fields during the fatigue cycles. A fracture mechanics-based fatigue model adopting the cyclic J-integral was here proposed, giving promising results for the interpretation of such failures.

Keywords: Shape memory alloy, biomedical device, cyclic behavior

* Corresponding author. Tel.: +39-02399-4307; fax: +39-02399-4286
E-mail address: lorenza.petrini@polimi.it

10.1016/j.prostr.2022.12.091

1. Introduction

Peripheral stenting is the clinical gold standard for the mini-invasive treatment of occlusive diseases affecting the arteries in the lower limbs. Stents are metallic grids that sustain the vessels through healing, allowing the correct blood perfusion. These stents are usually made of Nickel-Titanium (Ni-Ti), which belongs to the family of shape memory alloys (SMAs). At body temperature, Ni-Ti can be tailored to exploit superelasticity thanks to a reversible austenitic-martensitic phase transformation. Remarkably, it can recover elastically high deformations up to 8-10% (Maleckis et al., 2018). Superelasticity is exploited during the working life of Ni-Ti stents as they are manufactured through laser cutting from a tube, then crimped on the catheter (stent diameter reduces from 6-8 mm down to 2 mm) for the insertion into the body where the target lesion is located, without any permanent deformation. Successively, Ni-Ti stents are deployed and expand the vessel that, in turn, radially constrains the device inducing a preload. The leg movement causes a complex vessel deformation loading the stent repeatedly (on average, 10^6 cycles at 1 Hz combining axial compression, bending, and torsion act for one-year activity) (MacTaggart et al., 2014).

In the literature, peripheral stent fatigue failures are reported (Babaev et al., 2014) with possible dramatic drawbacks such as in-stent restenosis (Scheinert et al., 2005). For quality certification, new devices are required to survive up to 10^7 fatigue cycles (Auricchio et al., 2016; Li et al., 2010), that is 10 years of the equivalent activity. The standard approach requires the experimental verification of prototypes, according to the *testing for survival* strategy: following this, the stent integrity has to be proven after a fixed number of cycles under specified loading conditions, producing a failed/not failed output. Although this is an effective method, the time and cost of such campaigns are quite elevated and, for this reason, only a few different conditions can be proven. More recently, computational tools have been accepted to support the design and verification phases of new medical devices and much interest has been posed in their verification and validation to produce credible results (ASME, 2018). Indeed, numerical simulations provide an estimate of the impact of different loading conditions on the stent in terms of local stress and strain, at the computational cost only. Their results can be integrated with the experiments to provide a more complete picture to be used for interpretative and predictive purposes.

In the last years, given the lack of a specific framework for the fatigue assessment of Ni-Ti stents, a few studies were published by the authors' group on the topic of fatigue prediction in peripheral stents, following a phenomenological approach (Berti et al., 2021, 2019). In particular, numerical simulations of Ni-Ti stents undergoing multiaxial fatigue loads, mimicking the in vivo scenario, were run to investigate the local stress and strain fields. The results were post-processed using different multiaxial fatigue criteria to predict if and where failure occurs. Then, the real devices, corresponding to the numerical models, were experimentally tested: the comparison between in silico and in vitro results allowed to identify the most suitable criteria.

However, by observing the stent surfaces at high magnifications, it was possible to recognize multiple surface defects in the orders of few microns which acted as fracture initiators when failure was recorded. This fact suggested exploring the adoption of fracture mechanics principles to explain such failures (Urbano et al., 2015). This study aims to further investigate the possibility to adopt the cyclic J-integral, a non-linear crack driving force parameter, for the assessment of the fatigue life of Ni-Ti stent-like specimens.

2. Materials and methods

2.1. In-vitro and in-silico study

Experimental tests and computational simulations were combined to study the fatigue response of Ni-Ti multi-wire samples (Fig. 1a and 1c) constituted of nine wires with a gauge length of 15 mm and cross-section about 200 μm thick and 400 μm wide, compatible with the size of a stent strut. These samples were laser-cut from the same source tubes and underwent the same thermo-mechanical treatment typically adopted for stents, having the advantage to allow an easier evaluation of the stress-strain response of the material. Uniaxial fatigue tests were performed at 24 Hz in displacement control; a water environment at 37 °C was adopted to reproduce in vivo conditions (Fig. 1d). Each sample was pre-loaded applying a maximum strain above 6%, mimicking the stent crimping phase, followed by unloading till the fatigue valley, as in the stent deployment, and then subjected to fatigue load cycles at a certain level of mean strain and strain amplitude (Fig. 1e). Seven specimens were tested, each one under different conditions, with

the mean strain ranging between nominal 1% and 8% and strain amplitude up to nominal 2% (Table 1). The number of cycles to failure was recorded for each wire, assuming a run-out condition of 10^6 cycles (Pelton, 2011).

Finite element (FE) simulations mimicking the fatigue tests were carried out on the FE model reproducing the samples (Fig. 1b) to assess the stress-strain response in the gauge length of the wires in each test condition. All the simulations were performed in Abaqus 2020/Standard environment (Dassault Systems, SIMULIA Corp., RI) exploiting the available constitutive model for superelastic materials. The required model parameters, namely, Young's modulus of austenite and martensite (E_A, E_M), the stress levels defining the start and finish of the forward and the reverse transformation in tension ($\sigma^S_{tL}, \sigma^E_{tL}, \sigma^S_{tU}, \sigma^E_{tU}$), and the amplitude of the transformation plateau (ε^L) were calibrated from previous tests (Guala, 2018), while the Poisson's ratio of the austenite and martensite was taken from the literature (Berti et al., 2019) (Table 2). Using the stress-strain cycles obtained for each test condition from simulations, it was possible to draw a conventional strain-life diagram depicting the strain range against the interval of number of cycles to failure. Indeed, for each sample, one value of strain range and nine values of cycles to failure were collected.

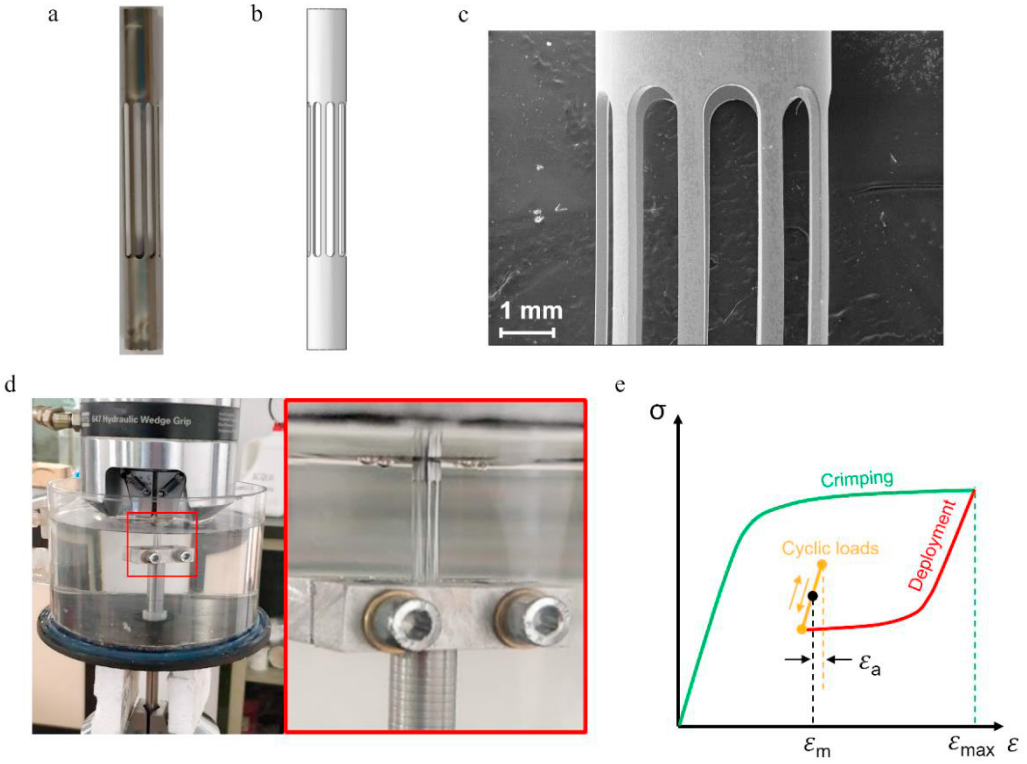

Fig. 1. (a) Multi-wire samples with nine parallel wires adopted in fatigue tests; (b) FE model of multi-wire samples; (c) SEM image of a multi-wire sample highlighting the geometrical features; (d) experimental set-up adopted for fatigue tests on multi-wire samples; (e) loading sequence applied to the samples resembling the stress and strain induced into the struts during stent implantation and working cycles: the sample is loaded up to a maximum deformation ε_{max} to simulate the crimping effect, then it is unloaded up to a lower strain, to account of the stent self-expansion into the vessel and partial deformation recovery, and then it is cyclically loaded around a mean strain value (ε_m) with a certain strain amplitude (ε_a) to replicate the stent fatigue cycles.

Table 1. Nominal values of mean strain ε_m and strain amplitude ε_a.

Sample	1	2	3	4	5	6	7
ε_m [%]	1	1.5	1.5	4	6	6	8
ε_a [%]	0.3	0.5	1	1	0.6	2	0.4

Table 2. Material parameters of Abaqus superelastic constitutive model.

E_A [MPa]	E_M [MPa]	σ^S_{tL} [MPa]	σ^E_{tL} [MPa]	σ^S_{tU} [MPa]	σ^E_{tU} [MPa]	ε^L [%]	ν_A [-]	ν_M [-]
40000	18000	200	250	80	45	4.9	0.3	0.3

2.2. Fracture mechanics-based life predictions

Beyond the conventional strain-life approach, a fracture mechanics-based crack driving force parameter was introduced to correlate experimental data accounting for the coupled effect of mean and amplitude strain on fatigue life. For this purpose, given the non-linear response of Ni-Ti alloy, the cyclic J-integral ΔJ was considered as this parameter was successfully applied in low cycle fatigue regimes for structural metallic alloys. Specifically, following the formulation reported by Patriarca et al. (Patriarca et al., 2018), the cyclic J-integral, assuming the plane stress condition given the limited thickness of the cross-section of the wires, can be computed as

$$\Delta J = Y^2 a\, \pi \left(\frac{\Delta\sigma^2}{E} + \frac{3}{4\sqrt{n'}}\, \Delta\sigma\, \Delta\varepsilon_{pl} \right). \tag{1}$$

The term in brackets in Equation (1) represents the sum of the elastic and plastic strain energy density of the cycle, where E (material elastic modulus) can be computed as the slope of the initial linear loading path, $\Delta\sigma$ is the stress range and $\Delta\varepsilon_{pl}$ is the plastic strain range. In these calculations, the material non-linear behavior was described by the Ramberg-Osgood equation (Fig. 2a), written as

$$\Delta\varepsilon = \Delta\varepsilon_{el} + \Delta\varepsilon_{pl} = \frac{\Delta\sigma}{E} + 2\left(\frac{\Delta\sigma}{2K'}\right)^{1/n'}, \tag{2}$$

where K' and n' are material-dependent hardening parameters. To correctly perform the fitting using Equation (2), the loading cycle has to be shifted to coincide with the origin of the $\Delta\sigma$-$\Delta\varepsilon$ axes. The fitting procedure was performed for all the seven samples by minimizing the difference between the sum of squared differences between the numerical and the analytical stress-strain curves, identifying all the necessary parameters (Fig. 2b). The computation of ΔJ also requires the knowledge of the defect length a and the boundary correction factor Y accounting for crack geometry, which were deduced from scanning electron microscope (SEM) observations. For each sample, all the failed wires were accurately analyzed, the area of the maximum defect was computed, and an equivalent radius approximating the crack length was derived.

The ΔJ was then used as the crack driving force parameter in a crack propagation algorithm. Following the approach reported by Haghgouyan et al. (Haghgouyan et al., 2021), a linear relationship was assumed between the ΔJ and the crack growth rate da/dN, assuming a modified Paris Law expressed as

$$\frac{da}{dN} = C'(\Delta J)^{m'}. \tag{3}$$

The material parameters m' and C' of Equation (3) (Table 3) were computed from the propagation curves reported by Stankiewicz et al. (Stankiewicz et al., 2006) representing the crack growth rate as a function of the stress intensity factor range ΔK obtained on $Ni_{50.8}Ti$ compact tension (C(T)) samples laser-cut from unrolled, flattened and shape-set thin-walled tube similar to that used in stents manufacturing. Considering that the present wire specimens underwent fatigue cycles at stress ratio R between about 0.2 and 0.7, the propagation curve at load ratio R=0.7 was considered and linearly fitted, the ΔJ was computed from the stress intensity factor as

$$\Delta J = \frac{\Delta K^2}{E}, \tag{4}$$

considering only the elastic contribution and assuming plane stress condition given the limited thickness of C(T) samples. An assumption of the elastic modulus E appearing in Equation (4) was made since Stankiewicz et al. (Stankiewicz et al., 2006) did not report the corresponding value: a value of 50 GPa was adopted.

The modified Paris Law was integrated from an initial crack size a_i up to a final crack size a_f to compute the number of cycles to failure through an iterative procedure. At each crack length, the ΔJ was computed according to Equation

(1), an arbitrary increment of the number of cycles *dN* was assumed and the correspondent crack advancement *da* was calculated. Both crack length and number of cycles were iteratively updated at each step till the final crack size was reached, obtaining the fatigue life. Different predictions were performed considering various values of initial crack length between 2 μm and 20 μm, while a final crack size equal to 150 μm was chosen from the fracture surfaces (Fig. 4a).

Table 3. Crack propagation parameters adopted for fatigue life predictions, computed from Stankiewicz et al. (Stankiewicz et al., 2006).

C' [(mm/cycle)/(MPa mm)$^{m'}$]	m' [-]
3.689×10^{-4}	1.863

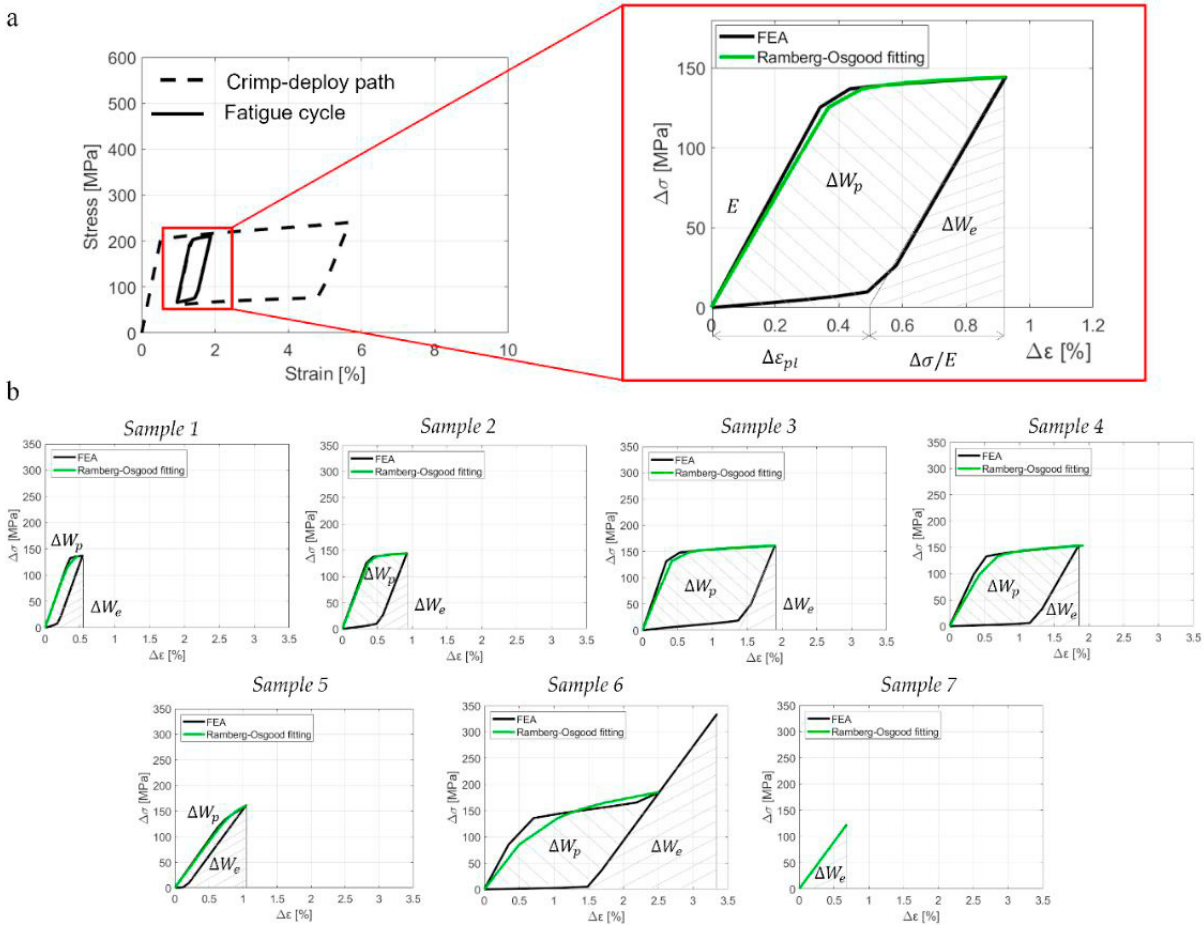

Fig. 2. (a) Example of a numerical stress-strain curve with indication of a fatigue cycle and a scheme of the fitting of the cycle with the Ramberg-Osgood equation: this allows to identify the elastic and plastic strain energy density (ΔW_e, ΔW_p) and compute the slope of the loading path (E), the elastic strain range ($\Delta\sigma/E$) and the plastic strain range ($\Delta\varepsilon_{pl}$). (b) Numerical fatigue cycle and fitting curve for all the seven samples with indication of elastic and plastic strain energy.

3. Results

3.1. In-vitro and in-silico study

The number of cycles to failure range recorded for each multi-wire sample in the experimental fatigue tests is reported in Table 4. The stress-strain cycles in the gauge length of the wires in each loading condition obtained through FE simulations are depicted in Fig. 2b on $\Delta\sigma$-$\Delta\varepsilon$ axes. In Fig. 3 the strain range evaluated from numerical $\Delta\sigma$-$\Delta\varepsilon$ curves is represented against the experimental number of cycles to failure, providing a conventional strain-life diagram.

3.2. Fracture mechanics-based life predictions

The results of the fitting procedure performed on numerical $\Delta\sigma$-$\Delta\varepsilon$ curves for all the seven samples are shown in Fig. 2b. The geometrical features of the maximum defect found on each sample are reported in Table 5 in terms of the square root of the area of the defect and its equivalent radius assuming a semi-circular shape. The initial size of the flaws ranges approximately from 1 μm to 25 μm. All the defects could be approximated as semi-circular surface flaws, adopting the simplified formulation of the boundary correction factor at the crack deepest point for a semi-infinite medium $Y=1.12\cdot(2/\pi)$.

The typical appearance of the fracture surface of failed wires is shown in Fig. 4a where both an initial flaw acting as a crack initiation site and the entire propagation region are highlighted, indicating the initial and the final crack length which were adopted in the calculations to estimate the number of cycles to failure. In Fig. 4b the predicted fatigue life is reported against the experimental number of cycles to failure for each wire, considering three initial crack lengths of 2 μm, 8 μm, and 20 μm corresponding to three different potential defect sizes. Both a safe and an unsafe region are highlighted to identify, respectively, conservative and non-conservative predictions with respect to experimental fatigue life.

Table 4. Minimum and maximum number of cycles to failure experimentally recorded on multi-wire samples.

Sample	1	2	3	4	5	6	7
$N_{f,min}$	6348	3384	1776	1800	8424	2376	27672
$N_{f,max}$	65568	8004	3672	4200	24180	2808	391728

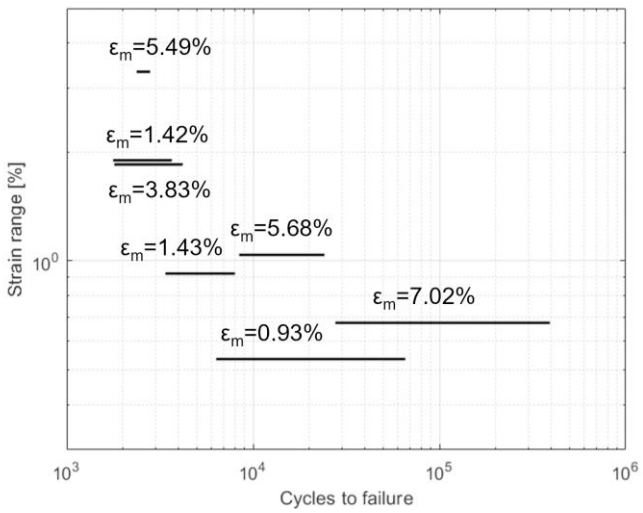

Fig. 3. Strain-life diagram depicting the strain range of the fatigue cycle against the number of cycles to failure for each sample, with indication of the mean strain value (ε_m) computed from FE curves.

Table 5. Geometrical features of maximum defects found on each multi-wire sample.

Sample	1	2	3	4	5	6	7
max $\sqrt{A}$ [μm]	2.40	31.62	1.40	2.47	2.94	7.99	1.43
r_{max} [μm]	1.91	25.23	1.12	1.97	2.35	6.37	1.14

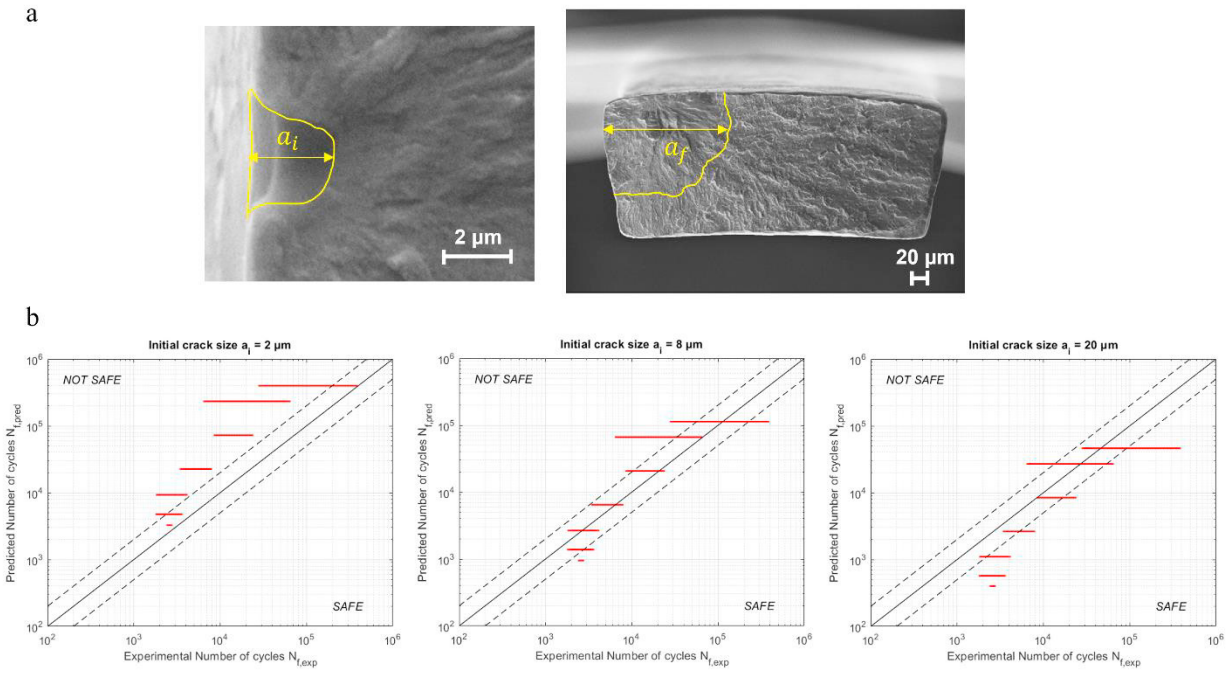

Fig. 4. (a) SEM image of the fracture surface of a failed wire with identification of the initial (a_i) and final (a_f) crack length; (b) representation of predicted fatigue life against experimental number of cycles to failure for all the samples considering three values of initial crack length.

4. Discussion and conclusions

The damage tolerant approach has not been yet widely used in the fatigue assessment of Ni-Ti cardiovascular devices, generally preferring those approaches devoted to avoid crack nucleation (Robertson et al., 2012). Indeed, some limitations have hindered the application of the damage tolerance approach such as, for example, the difficulty in obtaining crack growth data representative of the local microstructure of the Ni-Ti devices and the peculiar material's superelastic behavior preventing the usage of many principles formulated for standard metals.

This work represents a proof-of-concept study for the application of fracture mechanics methods for predicting Ni-Ti stent-like specimens' life. In SMAs different deformation regimes can be found according to the mean and amplitude strain values at the fatigue cycle. The non-linear fracture mechanics parameter cyclic ΔJ was herein introduced, and a crack propagation algorithm was calibrated according to crack growth rates data from literature and defect dimensions observed from the fracture surfaces. For structural metallic alloys, the cyclic ΔJ is computed from the hysteresis of elastic-plastic regimes in which dissipation phenomena occur during cycling. However, also SMAs exhibit hysteresis because of the energy exchange during the phase transformation and this promotes the adoption of the cyclic ΔJ as an appropriate crack driving force parameter.

This study demonstrates that the application of the cyclic ΔJ to the fatigue data gave promising fatigue life predictions in terms of the predicted number of cycles to failure. The authors acknowledge that the prediction is affected by the initial size of the defect, which appeared to be quite variable within the samples, while the choice of

the final defect size had a minor impact. More studies will be addressed to increase the knowledge of the Ni-Ti specific fracture properties, in the case of thin specimens for stent manufacturing.

Acknowledgments

The authors acknowledge Carlo Guala, PhD and Livanova for the experimental samples produced in its laboratory.

References

ASME, 2018. V&V 40: Assessing Credibility of Computational Modeling Through Verification and Validation: Application to Medical Devices.

Auricchio, F., Constantinescu, A., Conti, M., Scalet, G., 2016. Fatigue of Metallic Stents: From Clinical Evidence to Computational Analysis. Ann. Biomed. Eng. 44, 287–301. https://doi.org/10.1007/s10439-015-1447-8

Babaev, A., Hari, P., Zavlunova, S., Kurayev, A., 2014. Role of nitinol stent fractures in the development of in-stent restenosis in the superficial femoral artery. JACC Cardiovasc. Interv. 7, S35. https://doi.org/10.1016/j.jcin.2014.01.089

Berti, F., Spagnoli, A., Petrini, L., 2019. A numerical investigation on multiaxial fatigue assessment of Nitinol peripheral endovascular devices with emphasis on load non-proportionality effects. Eng. Fract. Mech. 216, 106512. https://doi.org/10.1016/j.engfracmech.2019.106512

Berti, F., Wang, P.J., Spagnoli, A., Pennati, G., Migliavacca, F., Edelman, E.R., Petrini, L., 2021. Nickel–Titanium peripheral stents: Which is the best criterion for the multi-axial fatigue strength assessment? J. Mech. Behav. Biomed. Mater. 113, 104142. https://doi.org/10.1016/j.jmbbm.2020.104142

Guala, C., 2018. The scientific and technological insights needed to design nitinol medical devices.

Haghgouyan, B., Young, B., Picak, S., Baxevanis, T., Karaman, I., Lagoudas, D.C., 2021. A unified description of mechanical and actuation fatigue crack growth in shape memory alloys. Acta Mater. 217, 117155. https://doi.org/10.1016/j.actamat.2021.117155

Li, J., Luo, Q., Xie, Z., Li, Y., Zeng, Y., 2010. Fatigue life analysis and experimental verification of coronary stent. Heart Vessels 25, 333–337. https://doi.org/10.1007/s00380-009-1203-9

MacTaggart, J.N., Phillips, N.Y., Lomneth, C.S., Pipinos, I.I., Bowen, R., Timothy Baxter, B., Johanning, J., Matthew Longo, G., Desyatova, A.S., Moulton, M.J., Dzenis, Y.A., Kamenskiy, A. V., 2014. Three-dimensional bending, torsion and axial compression of the femoropopliteal artery during limb flexion. J. Biomech. 47, 2249–2256. https://doi.org/10.1016/j.jbiomech.2014.04.053

Maleckis, K., Anttila, E., Aylward, P., Poulson, W., Desyatova, A., MacTaggart, J., Kamenskiy, A., 2018. Nitinol Stents in the Femoropopliteal Artery: A Mechanical Perspective on Material, Design, and Performance. Ann. Biomed. Eng. 46, 684–704. https://doi.org/10.1007/s10439-018-1990-1

Patriarca, L., Foletti, S., Beretta, S., 2018. A comparison of DIC-based techniques to measure crack closure in LCF. Theor. Appl. Fract. Mech. 98, 230–243. https://doi.org/10.1016/j.tafmec.2018.09.020

Pelton, A.R., 2011. Nitinol fatigue: A review of microstructures and mechanisms. J. Mater. Eng. Perform. 20, 613–617. https://doi.org/10.1007/s11665-011-9864-9

Robertson, S.W., Pelton, A.R., Ritchie, R.O., 2012. Mechanical fatigue and fracture of Nitinol. Int. Mater. Rev. 57, 1–37. https://doi.org/10.1179/1743280411Y.0000000009

Scheinert, D., Scheinert, S., Sax, J., Piorkowski, C., Bräunlich, S., Ulrich, M., Biamino, G., Schmidt, A., 2005. Prevalence and clinical impact of stent fractures after femoropopliteal stenting. J. Am. Coll. Cardiol. 45, 312–315. https://doi.org/10.1016/j.jacc.2004.11.026

Stankiewicz, J.M., Robertson, S.W., Ritchie, R.O., 2006. Fatigue-crack growth properties of thin-walled superelastic austenitic Nitinol tube for endovascular stents. J. Biomed. Mater. Res. Part A 79, 963–73. https://doi.org/10.1002/jbm.a.31100

Urbano, M.F., Cadelli, A., Sczerzenie, F., Luccarelli, P., Beretta, S., Coda, A., 2015. Inclusions Size-based Fatigue Life Prediction Model of NiTi Alloy for Biomedical Applications. Shape Mem. Superelasticity 1, 240–251. https://doi.org/10.1007/s40830-015-0016-1